Available online at www.elixirpublishers.com (Elixir International Journal)

Mechanical Engineering

Elixir Mech. Engg. 100 (2016) 43499-43503

ISSN: 2229-712X

Thermal Performance and Efficiency of a 6063 Aluminium Alloy Thermosyphon with Cerium IV Oxide Nanofluid using Response Surface Methodology

Alagappan.N and N. Karunakaran
Department of Mechanical Engineering, Annamalai University.

ARTICLE INFO

Article history:
Received: 4 October 2016;
Received in revised form:
2 November 2016;
Accepted: 9 November 2016;

Keywords
Optimization,
BBD,
RSM,
6063 AA TPCT,
Cerium IV Oxide Nanofluid.

ABSTRACT
The use of nanofluids as the operating fluid in the TPCT (two phase closed thermosyphon) significantly improves the heat transfer. In the present study, the performance enhancement of 6063 AA TPCT container material with cerium IV oxide nanofluid is investigated by RSM using Box-Behnken Design (BBD). According to BBD design, the process parameters are heat input (A), inclination angle of TPCT (B), and the flow rate of pure water in the condenser section (C). This work resulted in identifying the optimized set of input parameters and output response of the 6063 AA TPCT.

1. Introduction

The thermosyphon are very effective heat transfer devices employed to transmit large quantities of heat through a small cross-sectional area over a considerable distance with no additional power input to the system. They are also capable of controlling and transporting large quantities of heat at various temperature levels. They were first conceptualized in 1836 by Jocob Perkins and were called the perkins tube. The thermosyphon have been used in computers, solar systems, heat and ventilating air conditioning systems and many other applications [1].

Nanofluids possess unique properties, which motivate scientific community and industry to keep on intensive research of their fundamental aspects and practical applications. The most important properties of nanofluids are high thermal conductivity and low susceptibility of sedimentation, fouling, erosion and clogging as compare to ordinary fluids with micro particles. This inspired many promising applications of nanofluids, like those in nuclear energy, thermal management of systems with high dissipation rates of energy, cooling systems of electronic and optical devices.

Nanofluids enhance the heat transfer because (a) nanoparticles increase the thermal conductivity of the operating fluid, which eventually enhances the heat transfer efficiency of the TPCT [2,3] and (b) as the temperature increases, the Brownian motion of nano particles increases, which improves the convective heat transfer of the fluid [4,5]. The numerous studies have been reported concerning the nanofluid properties. Xuan et al., [6] presented a stable procedure for preparing nanofluids with emphasis on their heat transfer application.

Wen and Ding [7] experimentally studied on the convective heat transfer of nanofluids in a copper tube. Zhou[8] experimentally investigated on the heat transfer characteristics of copper nanofluids with any without acoustic cavitation. Chang[9] studied effects of the different volume concentrations of alumina nanoparticles on the boiling heat transfer characteristics of water with nanoparticles suspended. Ding and Wen[10] studied on the particle migration in pressure-driven laminar pipe flows of nanofluids. Koo and Kleinstreuer[11] considered the steady laminar liquid nanofluid flow in microchannels. Liu et al.,[12] investigated the thermal conductivity enhancement of ethyleneglycol and synthetic engine oil in the multiwalled carbon nanotubes. Yang et al.,[13] investigated the convective heat transfer co-efficients of nanofluids under laminar flow in a horizontal tube heat exchanger. Heris et al.,[14] investigated the laminar flow convective heat transfer of nanofluid in the circular tube with constant wall temperature boundary condition. Li et al.,[15] studied on the heat and mass transfer process of HFC134a gas hydrate in nano-copper suspension. Palm et al.,[16] numerically investigated on the heat transfer enhancement capabilities of coolants with suspended metallic nanoparticles inside typical radial flow cooling systems. Kang et al.,[17] experimentally investigated on the thermal performance of heat pipe with silver nano-fluid. He et al.,[18] studied on the heat transfer and flow behaviour of nanofluids flowing upward through a vertical pipe.

Basically this optimization process involves three major steps which are performing the statistically designed experiments, estimating the co-efficients in a mathematical model and predicting the response and checking the adequacy of the model[19]. The response surface methodology (RSM) is a statistical method that uses quantitative data from appropriate experiments to determine regression model equations and operating conditions[20]. A standard RSM design called Box-Behnken Design (BBD) was applied in this work. Not much work was found in the literature using 6063AA Thermosyphon. From the literature review it could be

Tele:
E-mail address: algatesmech06@gmail.com

concluded that the performance of a thermosyphon depended upon types of operating fluid, power input and inclination angle. The objective of this paper is to determine the efficiency and overall heat transfer co-efficient of 6063 AA TPCT filled with CeO_2 nanofluid.

2. Preparation of Nanofluid

The test nanofluid was obtained by dispersing CeO_2 nanoparticle in DI water at a concentration of 80mg/lit. Then the prepared sample was transferred into sonicator and sonicates upto 8 hrs with surfactant of ethylene glycol of 0.1% of volume of nanofluid.

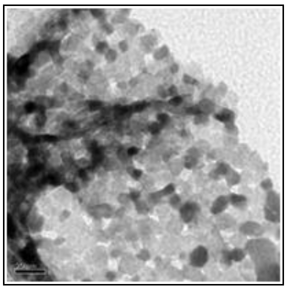

Fig 1. TEM image of Ceo_2.

Transmission Electron Microscope (TEM) analysis of the CeO_2 sample reveals an cubic crystalline morphology (Fig. 1) shows that nano-particles are well dispersed within base fluid. The mean size of the particles varies from 20-30 nm.

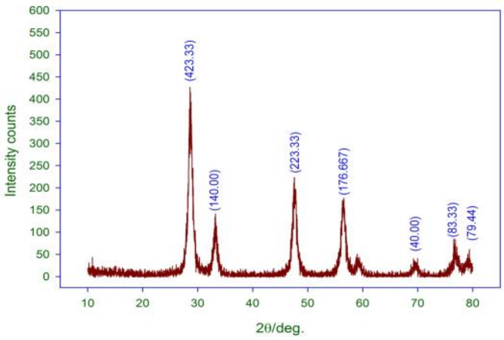

Fig 2. X-ray Diffraction Pattern.

To check the purity, we examined the nanoparticles with XRD tests. XRD pattern depicted in Fig.2.

The XRD profile established the perfect cubic crystalline nature of the cerium oxide nanoparticles. The high intensity peaks were observed at 423.33, 223.33, 176.667 crystal planes. The diffraction peaks in these XRD spectra indicate the pure cubic structure.

3. Experimental Setup

The system used for thermal performance measurement of TPCT is shown in Fig. 3

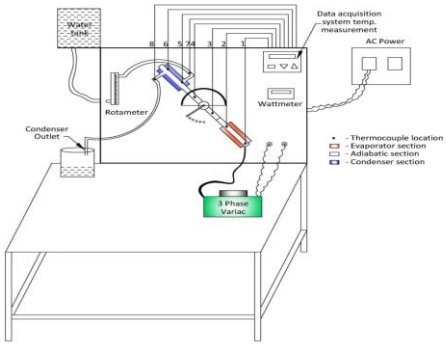

Fig 3. Experimental Setup.

The TPCT made of 6063 Aluminium Alloy tube with outer diameter of 12 mm, 2mm thickness and 750mm in length. The evaporator, the adiabatic and the condenser sections are uniformly 250mm length. The grade of the selected, TPCT container material was identified by conducting the chemical composition test. The result of chemical composition test is shown in table 1.

Table 1. Chemical composition (wt%) of Aluminium (AA6063) as container metal

Mg	Si	Fe	Cu	Mn	Zn	Cr	Al
0.7	0.532	0.35	0.1	0.7	0.02	0.1	Remainder

The experimental was carried out by BBD method in order to validate the RSM model. The BBD method employed with three parameters namely heat input (A), angle of inclination (B) and flow rate of pure water in the condenser section (C) over the output response of efficiency (η%) and overall heat transfer co-efficient ($U_{overall}$). Table 2 shows the process parameters and their levels. Table 3 shows the design of matrix.

The experimental was carried out by BBD method in order to validate the RSM model. The BBD method employed with three parameters namely heat input (A), angle of inclination (B) and flow rate of pure water in the condenser section (C) over the output response of efficiency (η%) and overall heat transfer co-efficient ($U_{overall}$). Table 2 shows the process parameters and their levels. Table 3 shows the design of matrix.

Table 2. Process parameters and their levels.

Parameters	Level		
	-1	0	1
A. Heat Input, W	90	120	150
B. Angle of inclination, °	30	60	90
C. Flow Rate, ml/min	100	150	200

Table 3. Design of Matrix.

Std	Run	Factor 1 A: Heat input	Factor 2 B: angle	Factor 3 C: flow Rate	Thermal efficiency (%)	Overall Heat Transfer Co-efficient ($U_{overall}$)
2	1	120	60	150	39.25	980.7
1	2	120	30	200	47.6	974.0
7	3	150	60	100	44.9	913.11
5	4	90	60	100	43.6	919.1
16	5	90	60	200	49.3	882.01
9	6	90	90	150	54.3	874.9
10	7	120	60	150	40.7	980.7
4	8	150	90	150	42.5	670.2
14	9	90	30	150	48.3	787.4
13	10	120	60	150	40.6	980.7
8	11	120	90	100	43.7	999.53
11	12	120	90	200	43.6	935.34
12	13	120	30	150	46.6	985.53
17	14	120	60	150	39.2	980.6
3	15	120	60	150	39.2	980.65
15	16	150	60	200	44.9	776.3
6	17	120	30	100	45.6	1083.94

The evaporator section of 6063 AA TPCT was heated with the plate type heater with a maximum power output of 200W and the condenser section was cooled by water with flow rate of maximum 200ml/min. The adiabatic section was insulated by glass wool to avoid the heat loss. The 6063 AA TPCT was charged with CeO_2 nanofluid at 50% of fill ratio. The wall temperature on the TPCT was measured by eight thermocouples of K-type. Two thermocouples were mounted on the evaporator section two on the adiabatic and four on the condenser section. All the thermocouples were connected and monitored using 8-channel data acquisition system (Countron-USB). The heater in the evaporator section was connected to the auto-transformer (III Phase). The heat input was varied by using variac which ranges between 90W-150W.

3.1. Test Procedure

The BBD simulations are arranged by 17 runs which is listed in table 3. The experiment starts with selecting the input variables and the response (output) that is to be measured.

The 17 runs of experiments depend on the input variables. At first the mass flow rate of pure water flowing through the condenser section was set using rotameter. The heat input incremented with the help of auto-transformer and the inclination angle of the TPCT. Approximately 6063 AA TPCT filled with CeO_2 attain the steady state at 20 minute in each of the 17 runs. The temperature at each trial was recorded after the attainment of the steady stake using data acquisition system (USB – Countron).

3.2. Data Reduction

The thermal efficiency of the thermosyphon (η%) is evaluated by,

$$\eta\% = \frac{Q_{out}}{Q_{in}} \quad (1)$$

$$Q_{out} = \dot{m}_c . c_p .(T_{out} - T_{in})$$

Where,

$\dot{m}_c$ = Mass flow rate of pure water in condenser section, kg/sec.

C_p = Specific heat of water, J/kg°C

T_{out} = Temperature at outlet of the water condenser section, °C

T_{in} = Temperature at inlet of the water condenser section °C

Q_{in} = Heat input in watts

The overall heat-transfer co-efficient (U) can be calculated by,

$$U_{overall} = \frac{Q_{in}}{\pi DL \ (\bar{T}_e - \bar{T}_c)} \quad (2)$$

where D and L are the diameter and the total length of the TPCT.

Table 4. ANOVA table for response 1.

Response	**Efficiency 1**					
ANOVA for Response Surface Quadratic Model						
Analysis of variance table [Partial sum of squares - Type III]						
	Sum of		**Mean**	**F**	**p-value**	
Source	Squares	df	Square	Value	Prob > F	
Model	263.5637	9	29.28485	42.93161	< 0.0001	Significant
A-HEAT INPUT	4.7337	1	4.7337	6.939608	0.0337	
B-ANGLE	18.97798	1	18.97798	27.82173	0.0012	
C-FLOW RATE	7.1442	1	7.1442	10.4734	0.0143	
AB	50.79072	1	50.79072	74.45923	< 0.0001	
AC	8.1225	1	8.1225	11.90759	0.0107	
BC	1.0609	1	1.0609	1.55528	0.2525	
A^2	100.0699	1	100.0699	146.7026	< 0.0001	
B^2	96.14287	1	96.14287	140.9455	< 0.0001	
C^2	0.52537	1	0.52537	0.770192	0.4093	
Residual	4.774895	7	0.682128			
Lack of Fit	2.284615	3	0.761538	1.223217	0.4101	Not Significant
Pure Error	2.49028	4	0.62257			
Cor Total	268.3386	16				

Table 5. ANVOA table for response 2.

Response	**U OVERALL 2**					
ANOVA for Response Surface Quadratic Model						
Analysis of variance table [Partial sum of squares - Type III]						
	Sum of		**Mean**	**F**	**p-value**	
Source	Squares	df	Square	Value	Prob > F	
Model	162962.8	9	18106.98	5352264	< 0.0001	Significant
A-HEAT INPUT	4377.65	1	4377.65	1293995	< 0.0001	
B-ANGLE	6356.654	1	6356.654	1878972	< 0.0001	
C-FLOW RATE	15140.61	1	15140.61	4475433	< 0.0001	
AB	12025.47	1	12025.47	3554624	< 0.0001	
AC	2486.02	1	2486.02	734845.8	< 0.0001	
BC	523.2656	1	523.2656	154672.8	< 0.0001	
A^2	76517.47	1	76517.47	22617899	< 0.0001	
B^2	2609.143	1	2609.143	771239.9	< 0.0001	
C^2	7120.817	1	7120.817	2104851	< 0.0001	
Residual	0.023681	7	0.003383			
Lack of Fit	0.015681	3	0.005227	2.613558	0.1881	Not Significant
Pure Error	0.008	4	0.002			
Cor Total	162962.8	16				

$\bar{T}_e$ and $\bar{T}_c$ are introduced as the average temperature of the evaporator and condenser sections, respectively.

4. Results and Discussion

From the above ANOVA table of 4 and 5, it is seen that, the F value for 6063 AA thermosyphon filled with CeO_2 is 42.93 which indicates that all the models are significant at 1 percent level. The values of less than 0.0500 indicate that the terms are significant at 5% level. In the response efficiency of 6063 AA TPCT with CeO_2 nanofluid B, C, AB, AC, A^2 and B^2 are significant at 1% level. The model terms are greater than 0.1 which indicates that they are not significant @ 1 percent and 5 percent level.

Similarly for the response $U_{overall}$, of 6063 AA TPCT with CeO_2 nanofluid, the F value is 5352264 which indicates that all the models are significant at 1 percent level. In this case all the model terms A, B, C, AB, AC, BC, A^2, B^2 and C^2 are significant at 1% level

4.1. Influence of various input parameters on thermal efficiency of 6063 AA TPCT with CeO_2 Nanofluid

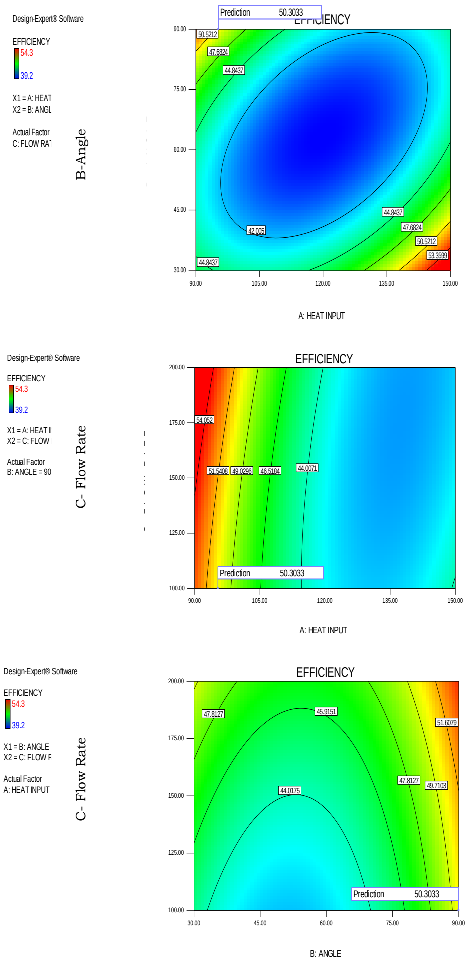

Fig 4. Influence of various input parameters on thermal efficiency.

The efficiency of 6063 AA TPCT filled with CeO_2 nanofluid was studied by pre-selected range of heat input and angle of inclination of TPCT. The results have been depicted in fig. 4. The results indicated that the maximum efficiency has been occurred in the high heat input and at maximum angle of inclination. Elliptical contour plot indicates the interactions between the heat input and angle of inclination are significant. This because of CeO_2 nanoparticle present in the DI water, achieves high efficiency due to the bombarding of vapour bubbles in the evaporator section and also high range of wettability was observed in the condenser section. During this heat transport takes place smoothly.

In case of heat input and flow rate the maximum efficiency is achieved at minimum heat input and at maximum flow rate. The lines of contour plot indicates that there no significant effect between Heat input and flow rate. Since the maximum efficiency achieve at minimum heat input causes, the evaporation of the fluid in the evaporator section at lower temperatures and the rapid transfer of heat to the maximum flow rate of pure water in the condenser section. Where as the interaction effect between angle of inclination and flow rate are also significant which is observed in the fig. 4.

The maximum efficiency is obtained at maximum inclination angle of TPCT and maximum of flow rate. As there is a considerable effect on the performance of the TPCT with angle of inclination and flow rate, because of reduction in contact surface between the container of TPCT and the heat transfer to the CeO_2 nanofluid. The heat loss associated in the exchange process to the pure water which is circulated in the condenser section.

4.2. Influence of various input parameters on overall heat transfer co-efficient of 6063 AA TPCT with CeO_2 nanofluid

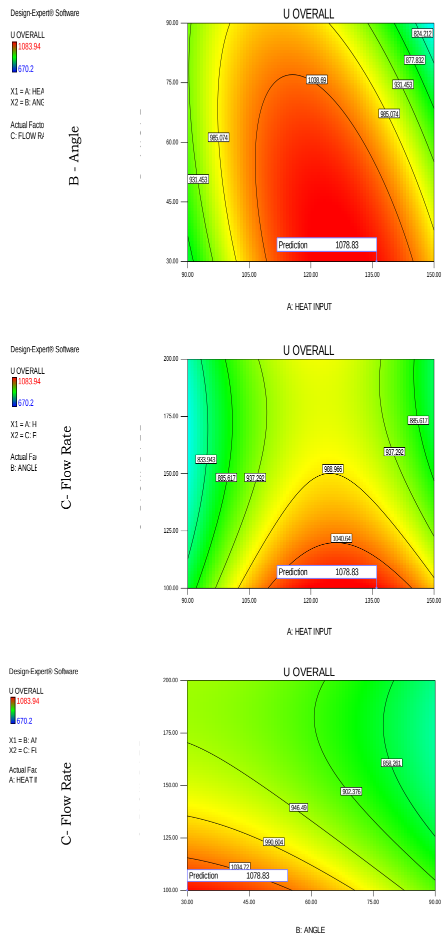

Fig 5. Influence of various input parameters on overall heat transfer co-efficient.

Fig. 5 shows the Heat input and inclination angle of TPCT are most important process parameters for assessing the high capacity of overall heat transfer co-efficient. The maximum value of 1078.83 $w/m^{2\circ}$ C occurs between 120W to 135W and the inclination of angle 75°. The contour plot indicates that there is significant effect due to the vigorous movement of vapour from the evaporator section to the condenser section. Thus the heat input and inclination angle have the remarkable impact on 6063 AA TPCT.

The high capacity of $U_{overall}$ is caused by the formation of vapour bubble of CeO_2 nanofluid at the liquid-solid interface. The Brownian motion dispersion and fluctuation of CeO_2 nanoparticles especially near the wall leads to increase in the high heat transfer rates. In other two cases of Fig. 5, the contour plot trends shows that there is no significant effect found between the selected input parameters. In first case increase in heat input increases the value of heat-transfer co-efficient to certain level and then decreases. The increase in flow rate significantly decreases the overall heat transfer co-efficient. The second case represents the increase of inclination angle decreases the heat transfer co-efficient and similar trend was found to flow rate also. The higher heat input decreases the fluid level in the evaporator section.

The optimized value for input parameters and output response were obtained using design expert software 8.0, which is given in table 6a&b.

Table 6a. Optimized input parameters.

Heat input	136.05 W
Angel	30^o
Flow rate	100.00 ml/min

Table 6b. Optimize Output Response.

η%	50.30%
$U_{overall}$	1078.83 $w/m^{2o}C$

Conclusion

The experimental investigations were carried out by BBD using RSM on the effect of various input parameters on the thermal performance of a 6063 AA TPCT, using CeO_2 nanofluid as the operating fluid, focusing on the efficiency and overall heat-transfer co-efficient.

Based on the experiments, the conclusions are as follows:

- CeO_2 nanofluid plays an important role in improving the thermal performance of 6063 AA TPCT.
- The proposed model will be useful to predict the thermal efficiency and overall heat transfer co-efficient.
- CeO_2 particle suspensions elevate the effective heat capacity. Hence the optimized value from RSM for overall heat transfer co-efficient was high (1078.83 $w/m^{2\circ}$ C)
- The optimized value from RSM for efficiency of 6063 AA TPCT was 50.3033%.
- The feasible optimum condition was 50.30% and 1078.83 $w/m^{2\circ}$ C which was very close to the predicted values 52.10% and 1051.2 $w/m^{2o}C$. Since the difference between the verification and predicted values was less than 5%, therefore the feasible optimum of the efficiency and overall heat transfer co-efficient was acceptable.

Nomenclature

CeO_2 - Cerium IV oxide nanoparticle
BBD - Box – Behnken Design
6063 - 6063 Aluminium Alloy Two
AA TPCT Phase Closed Thermosyphon
RSM - Response Surface Methodology
η% - Thermal Efficiency, %
U_{oerall} - Overall heat transfer co-efficient, $w/m^{2o}C$

References

1. A. Faghri, Heat Pipe Science and Technology, Taylor & Francis, 1995.
2. O.A. Alawi, N.A.C. Sidik, H. Mohammed, S. Syahrullail, Fluid flow and heat transfer characteristics of nanofluids in heat pipes: a review, Int. Commun. Heat Mass Transfer 56 (2014) 50–62.
3. M. Goodarzi, M.R. Safaei, K. Vafai, G. Ahmadi, M. Dahari, S.N. Kazi, N. Jomhari, Investigation of nanofluid mixed convection in a shallow cavity using a twophase mixture model, Int. J. Therm. Sci. 75 (2014) 204–220.
4. A. Malvandi, D. Ganji, Brownian motion and thermophoresis effects on slip flow of alumina/water nanofluid inside a circular microchannel in the presence of a magnetic field, Int. J. Therm. Sci. 84 (2014) 196–206.
5. A. Malvandi, M.R. Safaei, M.H. Kaffash, D.D. Ganji, MHD mixed convection in a vertical annulus filled with Al2O3–water nanofluid considering nanoparticle migration, J. Magn. Magn. Mater. 382 (2015) 296–306.
6. Y. Xuan, Q. Li, Heat transfer enhancement of nanofluids, Int. J. Heat Fluid Flow 21 (2000) 58–64.
7. D. Wen, Y. Ding, Experimental investigation into convective heat transfer of nanofluids at the entrance region under laminar flow conditions, Int. J. Heat Mass Transf. 47 (2004) 5181–5188.
8. D.W. Zhou, Heat transfer enhancement of copper nanofluid with acoustic cavitation, Int. J. Heat Mass Transf. 47 (2004) 3109–3117.
9. I.C. Bang, S.H. Chang, Boiling heat transfer performance and phenomena of Al2O3– water nano-fluids from a plain surface in a pool, Int. J. Heat Mass Transf. 48 (2005) 2407–2419.
10. Y. Ding, H. Alias, D. Wen, R.A. Williams, Heat transfer of aqueous suspensions of carbon nanotubes (CNT nanofluids), Int. J. Heat Mass Transf. 49 (2006) 240–250.
11. J. Koo, C. Kleinstreuer, Laminar nanofluid flow in microheat-sinks, Int. J. Heat Mass Transf. 48 (2005) 2652–2661.
12. M.S. Liu, M.C.C. Lin, I.T. Huang, C.C. Wang, Enhancement of thermal conductivity with carbon nanotube for nanofluids, Int. Commun. Heat Mass Transf. 32 (2005) 1202–1210.
13. Y. Yang, Z.G. Zhang, E.A. Grulke, W.B. Anderson, G. Wu, Heat transfer properties of nanoparticle-in-fluid dispersions (nanofluids) in laminar flow, Int. J. Heat Mass Transf.
48 (2005) 1107–1116.
14. S.Z. Heris, S.G. Etemad, M.N. Esfahany, Experimental investigation of oxide nanofluids laminar flow convective heat transfer, Int. Commun. Heat Mass Transf. 33 (2006) 529–535.
15. J. Li, D. Liang, K. Guo, R. Wang, S. Fan, Formation and dissociation of HFC134a gas hydrate in nano-copper suspension, Energy Convers. Manag. 47 (2006) 201–210.
16. S.J. Palm, G. Roy, C.T. Nguyen, Heat transfer enhancement with the use of nanofluids in radial flow cooling systems considering temperature-dependent properties, Appl. Therm. Eng. 26 (2006) 2209–2218.
17. S.W. Kang, W.C. Wei, S.H. Tsai, S.Y. Yang, Experimental investigation of silver nanofluid on heat pipe thermal performance, Appl. Therm. Eng. 26 (2006) 2377–2382.
18. Y. He, Y. Jin, H. Chen, Y. Ding, D. Cang, H. Lu, heat transfer and flow behaviour of aqueous suspensions of TiO2 nanoparticles (nanofluids) flowing upward through a vertical pipe, Int. J, Heat Mass Trans 50 (2007) 2272–2281.
19. D. Krishna, K. Siva Krishna and R. Padma Sree, Response surface modeling and optimization of chromium (vi) Removal from aqueous solution using Borrasus flabellifer coir powder, Int. J. of Applied Science and Engineering. 2013, (213-226).
20. Montgomerry D.C. 2001. “Design and Analysis of Experiments” 5th ed., John Wiley Sons, New York, USA.